energy&fuels

Article

Cite This: Energy Fuels 2019, 33, 5664−5672

pubs.acs.org/EF

Ignition Study of an Oxygenated and High-Alkene Light Petroleum Fraction Produced from Automotive Shredder Residues

S. Tipler,*[,†,‡,§] C. S. Mergulhão,[∥] G. Vanhove,[∥] Q. Van Haute,[⊥] F. Contino,[‡,§] and A. Coussement[†,§]

[†]Aero-Thermo-Mechanics Laboratory, Ecole Polytechnique de Bruxelles, Université Libre de Bruxelles, B-1050 Bruxelles, Belgium

[‡]Department of Mechanical Engineering, Vrije Universiteit Brussel, B-1050 Bruxelles, Belgium

[§]Combustion and Robust Optimization Group (BURN), Université Libre de Bruxelles and Vrije Universiteit Brussel, B-1050 Bruxelles, Belgium

[∥]Univ. Lille, CNRS, UMR 8522-PC2A-Physicochimie des Processus de Combustion et de l'Atmosphère, F-59000 Lille, France

[⊥]Comet Traitement, Rivage de Boubier 25, B-6200 Châtelet, Belgium

Supporting Information

ABSTRACT: Waste to energy is a key driver to achieve a clean and virtuous renewable cycle. Among others, the processes to convert organic matter in wastes from automotive residues, mainly composed of rubbers and foams [ethylene propylene diene monomer (EPDM) and polyurethane (PUR)], polyolefin plastics [polypropylene (PP) and polyethylene (PE)], styrenic plastics [acrylonitrile butadiene styrene (ABS) and polystyrene (PS)], and other thermoplastics [polyvinyl chloride (PVC) and polycarbonate (PC)], into a liquid fuel are now reliable. This new, atypical, and uncharted fuel is expected to emit large levels of pollutants, bringing new challenges that must be resolved by the combustion community. Advanced combustion modes appear to be a solution to enhance the efficiency and cutoff the NO_x and soot particle emissions. The present paper addresses the scarcity of experimental data by investigating the autoignition in a rapid compression machine. The pressure and temperature were swept from 10 to 20 bar and from 700 to 880 K, respectively, and the equivalence ratio was equal to 0.5. These conditions match with the homogeneous charge compression ignition (HCCI) mode operating with exhaust gas recirculation, especially for the low to intermediate (intermediate to high) temperature (pressure). The studied fuel is the light fraction of the synthetic crude oil, described by high-alkene and high-oxygenate levels. Several specificities have been detected: a limited low-temperature reactivity and a low negative temperature coefficient. Combustion simulation will be carried out in further work to determine to what extent advanced combustion modes will play a role to achieve a clean combustion in a waste-to-energy perspective.

INTRODUCTION

During the last 4 years of decline, the number of end-of-life vehicles in the European Union (EU) was converging and remained nearly constant from 2012 to 2015 with an average of 6 million units.[1] Recycling is an answer to mitigate the environmental impact of wastes produced from end-of-life vehicles, but at the end of a conventional recycling process, up to 20% of the initial mass remains.[2,3] Some advanced processes can reach levels as low as 7%.[4] These leftover products, called automotive shredder residues (ASRs), are composed of rubbers and foams [ethylene propylene diene monomer (EPDM) and polyurethane (PUR)], polyolefin plastics [polypropylene (PP) and polyethylene (PE)], styrenic plastics [acrylonitrile butadiene styrene (ABS) and polystyrene (PS)], and other thermoplastics [polyvinyl chloride (PVC) and polycarbonate (PC)],[5] which makes them good candidates to be converted into liquid fuels burned in a combined heat and power engine.

A fuel produced from ASRs shows a different composition than conventional fuels. Gasoline is traditionally mainly composed of paraffins (30−70%) and aromatics (20−45%), with the remaining molecules being olefins (5−20%).[6,7] In ASRs, a higher amount of olefins (around 30%) than the limit requested by the European Directive 2009/30/EC[8] is induced by straight polymers, such as PE or PP.[9,10] This limit is required as a result of the formation of aromatic ring soot particle emissions and butadiene, which is registered as a toxic substance.[11]

A high oxygenate fraction (around 15%) is due to oxygenated polymers, such as PC and polyamide, as well as the substitution of heteroatoms by −OH radicals during the fuel treatment process.[12]

Because the paraffinic fraction and the hydrogen/carbon mole ratio (H/C) are low, waste-derived fuels emit high levels of pollutants (nitrogen oxides, partially oxidized products, and soot particle emissions). Mani et al.[13] explained these high concentrations by the high flame temperature of substituted and cyclic molecules and poor mixing capabilities with the formation of local rich areas in the cylinder. Combustion considerations should also be investigated to compare the soot formation and consumption rates. Kumar et al.[14] observed similar trends and drew the same conclusions. Clean combustion modes emerge as being the keystone to make these lower grade fuels acceptable for society.

Received: March 4, 2019
Revised: May 17, 2019
Published: May 24, 2019

DOI: 10.1021/acs.energyfuels.9b00649
Energy Fuels 2019, 33, 5664−5672

Homogenous charge compression ignition (HCCI), where a homogeneous reacting mixture is compressed until autoignition, has already proven its potential in reducing the nitrogen oxides and the soot particle emissions in the exhaust gases thanks to a better mixing between the air and the fuel, thus reducing the in-cylinder peak temperatures and locally rich areas.[15−18] This combustion mode was tested with alternative fuels, including low-octane gasolines,[18] valeric biofuels,[15] biomass,[16] and ammonia.[17,19,20] Nonetheless, the low-temperature combustion of fuels derived from ASRs is still uncharted.

HCCI has no direct ignition control because the mixture is prepared before the closure of the intake valves, without an in-cylinder injection. The ignition is extremely sensitive to the initial and compressed conditions [the chemical composition and the temperature and pressure at top dead center (TDC)] because it is controlled by the kinetics. This last remark is a major barrier for the development of HCCI applied to ASR-derived fuels as a result of the fluctuation of their composition and properties when the raw matter is modified.

More precisely, this inconstancy is problematic if the variation of the ignition delay (ID) is not considered. On the one hand, a too short ID could lead to early ignition with very high heat release rates damaging the piston. On the other hand, a fuel that is not reactive enough could lead to misfires. As a solution, the fuel ignition at TDC could be investigated with a numerical model to adapt the engine operating conditions, with the conditioning of the initial temperature, exhaust gas recirculation rate, and equivalence ratio. Performing simulations of a fuel made up of hundreds of molecules is unfortunately unrealistic in terms of computational complexity. Instead, a surrogate fuel, mixture of about 2−10 molecules traditionally generated and validated on the basis of experiments,[21−29] could substitute the real fuel.

This research aims at gathering experimental data to later formulate a surrogate, together with addressing the lack of information regarding the reactivity of fuels produced from ASRs, which are still uncharted. HCCI-like conditions were investigated in a rapid compression machine (RCM) to measure IDs, defined as the measured time between the TDC and the maximum pressure derivative value. After the methodology has been described to characterize the light fraction derived from ASRs, its autoignition will be discussed with respect to the temperature and pressure at TDC to point out the usual and atypical aspects of its ignition characteristics.

This first study will be used as a baseline for formulating a surrogate fuel to perform numerical investigations and is a step forward for the reduction of pollutant emissions from waste-derived fuels via advanced combustion modes.

EXPERIMENTAL SECTION

Fuel Characterization. Fuel classification is important because similar fuels tend to show similar characteristics, while their differences explain their properties and specificities. The studied fuel is known as a light fraction, but its composition depends upon the raw matter and the production parameters. The distillation curve was measured according to the ASTM International Standard D86 to compare it to the typical classes of fuels: gasoline, naphtha, kerosen, or diesel.

The distillation profile almost coincides with the profile of a heavy naphtha (see Figure 1), except for the 10 last volume fractions, where higher temperatures are required to reach the same evaporation extent. Therefore, the molecules are expected to be longer and more saturated than in a conventional gasoline.

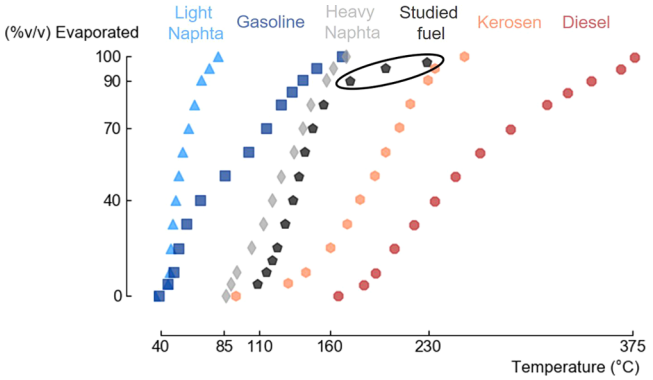

Figure 1. Typical atmospheric distillation ranges of distillation fractions according to the ASTM International Standard D86. The studied fuel is comparable to a heavy naphtha, except for the last 10 vol %. The distillation curves of the different classes of fuels were published by Chang et al.[30,31]

The octane numbers (ONs) [research octane number (RON), ASTM D2699; motor octane number (MON), ASTM D2700] are important parameters that denote the resistance of a fuel toward end-gas knock. They provide information on the fuel reactivity under two conditions and are often used as target properties to formulate a surrogate fuel.[23−25] ASTM D2699 and D2700 rely on a certified engine, but a low volume of fuel was available; therefore, it was not possible to measure the octane numbers. Correlations to predict the octane rating from ignition delay times exist,[32−34] but they have never been tested within the ranges of the ASR fuel chemical fraction and could not be applied in the case of this type of fuel, which shows long molecules and high concentrations of olefin, alcohols, ketones, and other oxygenates. Therefore, these correlations would have led to an approximated octane index without the knowledge of a confidence interval.

From a kinetic point of view, the difference between the RON and MON, usually known as the sensitivity, can be assumed to be correlated with the difference in reactivity in the low- and intermediate-temperature ranges.[35] However, comparing measurements of ignition delays to octane number is not straightforward, even though correlation exists.[36]

The separation between both of these temperature domains is usually associated with the negative temperature coefficient (NTC) behavior, where the global reactivity toward autoignition decreases as the compressed temperature increases. It is widely accepted that, at low temperatures, the reactivity is dominated by chain-branching pathways relying on the addition of O_2 to radicals formed from the parent fuel molecules. In the NTC temperature range, these pathways compete with non-chain-branching pathways, forming unsaturated species (i.e., an alkene if the fuel is an alkane).[35,37−39] The intensity of the NTC, i.e., the slope of the ignition delay according to the compressed temperature under intermediate temperature, is of crucial importance to predict the behavior of one fuel in HCCI.[40]

The ASR fuel was analyzed at Ghent University with comprehensive two-dimensional gas chromatography (GC × GC) coupled with a flame ionization detector and time-of-flight-mass spectrometry to obtain the *n*-paraffin, iso-paraffin, olefin, naphthene, aromatic, and oxygenate (PIONAOx) distribution[12,41,42] (Table 1). The signal of ketones and aromatics overlapped; therefore, a correction was applied to revise the overestimated aromatics and underestimated oxygenates.[12] Other hydrocarbon types identified in minor quantities, namely, naphthenaromatics, nitrogenates, diaromatics, and sulfurates, have been neglected in the present work. The whole composition is available in the Supporting Information. GC × GC revealed only 16.5% of paraffins (normal and iso) in the fuel, where, usually, paraffins account for more than 35%. The mean number of carbon atoms was nine for all of the groups (C9), except the aromatics (C8) and oxygenates (C6), whereas gasoline usually exhibits C7−C8 molecules. It is noteworthy that the gasoline

DOI: 10.1021/acs.energyfuels.9b00649
Energy Fuels 2019, 33, 5664−5672

Table 1. *n*-Paraffin, Isoparaffin, Aromatic, Olefin, Naphthene and Oxygenate (PIONAOx) Mole Fractions of the Studied Fuel Compared to Other Light Fuels from the Literature: Fuels for Advanced Combustion Engine (FACE) A, C, F, G, I, and J, a Gasoline Provided by Haltermann (HG) and Another by Coryton (CG), a Saudi Aramco Light Naphtha (SALN), and a Haltermann Straight Naphtha (HSN)[25−29,43 a]

(%, mol/mol)	P	I	O	N	A	Ox
studied fuel	4.86	11.63	29.61	12.95	24.95	16.00
overall ranges	(4.80, 55.78)	(26.10, 83.70)	(0.00, 11.20)	(1.50, 15.80)	(0.30, 33.60)	(0.00, 16.80)
FACE A	13.20	83.70	0.40	2.40	0.30	0.00
FACE C	28.60	65.10	0.40	1.50	4.40	0.00
FACE F	4.80	61.00	10.00	15.80	8.40	0.00
FACE G	7.90	38.30	7.90	14.10	31.80	0.00
FACE I	14.00	70.00	7.00	4.00	5.00	0.00
FACE J	31.50	32.40	0.60	2.40	30.60	0.00
HSN	36.70	37.80	0.00	15.00	10.50	0.00
SALN	55.40	35.90	0.00	6.70	1.32	0.00
HG fuel	12.20	26.10	6.30	15.60	22.90	16.80
CG fuel	10.10	31.90	11.20	5.00	33.60	8.20

[a]Fuels with different features were selected, including atypical fuels, to show the specificities of the studied fuel. HG fuel is the most similar fuel to the studied fuel, with a low paraffin fraction and high olefin and oxygenate fractions.

Table 2. Properties of the Studied Fuel Compared to Other Light Fuels from the Literature: Fuels for Advanced Combustion Engine (FACE) A, C, F, G, I, and J, a Gasoline Provided by Haltermann (HG) and Another by Coryton (CG), a Saudi Aramco Light Naphtha (SALN), and a Haltermann Straight Naphtha (HSN)[25−29,43 a]

	H/C	MW (g/mol)	density (kg/m^3) at 15 °C	RON	sensitivity
studied fuel	1.80[12]	120 ± 3[44,45]	796.1[46]		
overall ranges	(1.78, 2.34)	(78.40, 100.2)	(642, 760)	(60.00, 96.8)	(−0.1, 11.0)
FACE A	2.29	97.80	685.3	83.5	−0.1
FACE C	2.27	97.20	690.5	84.7	1.1
FACE F	2.13	94.80	707.0	94.4	5.6
FACE G	1.83	99.70	760.0	96.8	11.0
FACE I	2.24	95.50	688.0	70.3	0.7
FACE J	1.91	100.2	741.0	71.8	3.0
HSN	2.15	92.41	705.0	60.0	1.7
SALN	2.34	78.40	642.0	64.5	1.0
HG fuel	1.97	88.80		91.0	7.6
CG fuel	1.78	90.60		97.5	10.9

[a]Fuels with different features were selected, including atypical fuels, to show the specificities of the studied fuel. FACE G is the most similar fuel to the studied fuel with a low HC ratio, a high MW, but a relatively low density compared to FACE G.

provided by Haltermann and studied by Lee et al. has a similar composition to the studied fuel, where some olefins are basically substituted by paraffins[43] (Table 1).

The elemental composition was measured with an elemental analyzer and GC × GC, associated with a nitrogen chemiluminescence detector and a sulfur chemiluminescence detector.[12,41,42] The low H/C ratio and high density of the studied fuel indicate the high quantity of aromatics and saturated compounds, while the high molecular weight (MW), estimated with the Lee−Kesler method,[44,45] is a consequence of long molecules. The MW uncertainty was estimated on the basis of the literature, as explained thereafter. Riazi compared the errors on the estimated MWs of five fuels (from 233 to 523 g/mol).[44] The Lee−Kesler method was particularly accurate for the two fuels with the lowest MWs (233 and 267 g/mol, estimated with an error of −1.3 and −0.3 g/mol, respectively). Therefore, the uncertainty was estimated to be ±3 g/mol. FACE G is the most similar fuel from the recent literature in terms of properties, with a similar HC ratio, a high MW, and a high density (Table 2).

RCM. To gain insight on the reactivity of the fuel in both temperature regimes, ignition delays were measured in the Université de Lille RCM, which had been extensively described in previous studies.[39,47,48] The RCM is based on a right-angle design, in which a moving cam imposes the movement of the compressing piston, therefore ensuring strictly constant volume of the combustion chamber after the compression as well as reproducibility of the compression phase. In this study, the volumetric compression ratio was 10.3:1 and the compression time was 45 ms. The end of compression time was determined with an optocoupler fixed on the moving piston facing a comb with a 1 mm resolution. A creviced piston is used to mitigate piston corner vortex formation during the compression phase,[49] ensuring temperature homogeneity during the ignition delay period. The tests were carried out under pressures ranging from 10 to 20 bar at TDC and at an equivalence ratio of 0.5 to study lean conditions, which is a feature of the HCCI mode. In this mode, the equivalence ratio generally ranges from 0.3[15−20] to 0.8[50−52] with a high EGR rate. Measurements for stoichiometric mixtures would not have made sense in the context of HCCI application, while the validity of kinetic mechanisms for very lean mixtures can sometimes be limited. Therefore, an equivalence ratio of 0.5 represents a meaningful compromise.

The compressed temperature is inferred from the measurements of initial temperature and pressure, and the compressed pressure is inferred using the isentropic law under the adiabatic core assumption. It is varied by changing the composition of the diluent in the mixture, with N_2, Ar, and CO_2 being used. Non-reactive mixtures were tested as well, and the volume profiles are supplied in the Supporting Information.

Despite its global low MW, the fuel was composed of a small portion of heavy molecules. A gas chromatography/mass spectrometry (GC/MS) analysis of the liquid fraction obtained after

DOI: 10.1021/acs.energyfuels.9b00649
Energy Fuels 2019, 33, 5664−5672

evaporation at 85 °C from 0 to 1.14 kPa revealed molecules with up to 20 carbon atoms.

These molecules can potentially explain the change of slope corresponding to the heaviest in the distillation curve (Figure 1). The fraction of heavy compounds present in the fuel is likely to be problematic for HCCI application; however, the fuel production process is still under development, so that the identified heavy molecules will be removed in the future to avoid evaporation and impingement issues. To ensure the repeatability of the mixture preparation, the initial liquid volume of fuel, mixture preparation temperature, and evaporation time were kept constant.

The fraction of the fuel that may have been evaporated was estimated, but a precise evaporation simulation with Antoine's equation and Raoult's law cannot be realized as a result of the complexity of the fuel. To circumvent this issue, a confidence interval for the quantity of fuel that was evaporated was estimated. To define a subset of the more volatile molecules that would have been evaporated, the boiling points under atmospheric conditions of the molecules detected by GC × GC were compared to a predefined limit to estimate if they were likely to evaporate. The indicative threshold was chosen to be equal to 216 °C, the boiling point of *n*-dodecane under atmospheric conditions, because this molecule has a boiling point (86 °C at 8.55 Torr) of the same order of magnitude as the temperature of the mixing chamber (85 °C at 8.55 Torr). With each molecule evaporation being governed by Raoult's law, the fraction that was effectively evaporated is assumed to be between the whole fuel and the sum of the fractions of the molecules that would have been evaporated in the worst case scenario (93.6% in mass).

The fuel heat capacity was estimated on the basis of the molecules identified with GC × GC and considering the molecules that may have not been evaporated according to the subsequent procedure. With each molecule being governed by Raoult's law, the heat capacity of the fuel that was effectively evaporated was assumed to be between the heat capacity of the total fuel and the heat capacity of the mixture, where only the more volatile molecules would have been evaporated. For some species, only the raw formula was determined; therefore, the maximal and minimal values were selected from a set of molecules with the same atomic composition to define a confidence interval for the heat capacity of each fuel. As a result, the heat capacity of the evaporated fuel is between those of the reduced and total fuels, which defines the confidence interval. The half-width temperature uncertainty was defined on the basis of the two compressed temperatures calculated with the minimal and maximal values of the specific heat. This uncertainty, resulting of the heat capacity only, remains low (1.5−3.5 K) because the mixture heat capacity mainly depends upon the oxygen and diluent concentrations.

The final NASA coefficients under low temperatures (0−1000 K) and the compositions of the studied mixtures defining the minimal and maximal heat capacities are reported in the Supporting Information.

The confidence interval is localized between the heat capacity of representative molecules of each hydrocarbon group (Figure 2). This can be explained by the fact that PIONAOx is well-divided between groups, showing a high and low heat capacity. The influence from aromatics and olefin compensates for each other because both classes have similar concentrations; this is also true for ketones and naphthenes. It is noteworthy that the studied fuel shows a rather high heat capacity because two groups out of six, i.e., aromatics and ketones, have a low heat capacity. A simple primary reference fuel (PRF) blend composed of iso-octane and *n*-heptane would not be able to correctly capture the heat capacity in the studied temperature range. Adding toluene would decrease the heat capacity; therefore, a toluene reference fuel (TRF) would not improve the representability of the surrogate. However, a simple surrogate fuel composed of the selected representative molecules blended according to the fuel PIONAOx fraction (Table 1) shows a heat capacity that falls near the confidence interval.

The pressure at TDC was set by controlling the initial pressure of the mixture. The mixtures were prepared using the partial pressure method in a mixture preparation facility heated at 85 °C. The

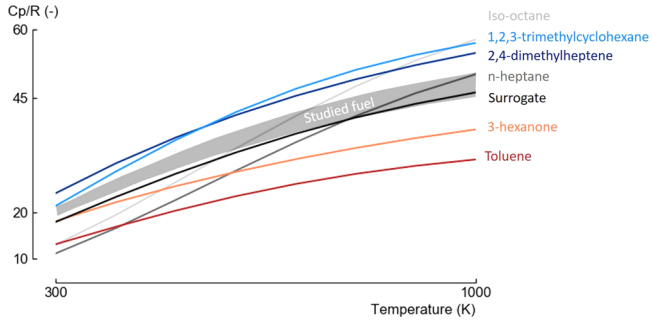

Figure 2. Confidence interval of the studied fuel heat capacity compared to representative molecules for each hydrocarbon group. A surrogate fuel composed of the six plotted molecules blended according to the PIONAOx fraction reported in Table 1 is also considered.

theoretical equivalence ratio depends upon the atomic mass fractions (measured with an elemental analyzer and GC × GC coupled with a nitrogen chemiluminescence detector and a sulfur chemiluminescence detector[12,42]) and the measured partial pressures during the mixture preparation.

The propagation of uncertainty (following the Joint Committee for Guides in Metrology recommendations[53]) leads to the calculation of the accuracy on the equivalence ratio. The atomic mass fractions and the partial pressure standard uncertainties were calculated on the basis of their standard deviations and the specifications of the manufacturer with a rectangular distribution, respectively. A correction factor of 3 was chosen to obtain an estimation at 99% of the confidence interval, defined by the expanded uncertainty. As a result, $u(\phi) = 0.15\%$; therefore, $\phi = 0.5 \pm 0.0045$.

Numerical Simulation. Numerical simulations were carried out to compare the ASR fuel reactivity to two fuels among those identified in Table 2. FACE G shows a high RON (RON = 96.8) and a high sensitivity ($s = 7.9$) conversely to FACE I (RON = 70.3, and $s = 0.7$) and their ignition delays are dissimilar.[26,27] FACE G has a lower reactivity than FACE I. Moreover, they were already tested with the same kinetic mechanism; therefore, the just cited fuels were selected to define a frame of reference to discuss the ASR fuel ignition delays. The compositions of FACE G and I surrogates proposed by King Abdullah University of Science and Technology (KAUST) are listed in Table 3.

Table 3. Composition of the FACE Gasoline G and I Multicomponent Surrogates Proposed by KAUST

(%, mol/mol)	FGG-KAUST[26]	FGI-KAUST[27]
n-butane	7.6	
n-heptane		12
2-methylbutane	9.5	11
2-methylhexane	9.8	27
2,2,4-trimethylpentane	18	34
1-hexene	8.1	6
cyclopentane	15.3	6
1,2,4-trimethylbenzene	21.1	4
toluene	10.6	

Simulations of a variable volume batch reactor were carried out with Cantera and the FACE gasoline kinetic mechanism.[26] The volume profile was inferred from the non-reactive pressure profile with an isentropic law assumption as described by Bourgeois et al.[54] With this method, an additional volume expansion term accounts for the effective heat losses after the end of compression. The non-reactive volume profiles are reported in the Supporting Information.

DOI: 10.1021/acs.energyfuels.9b00649
Energy Fuels 2019, 33, 5664−5672

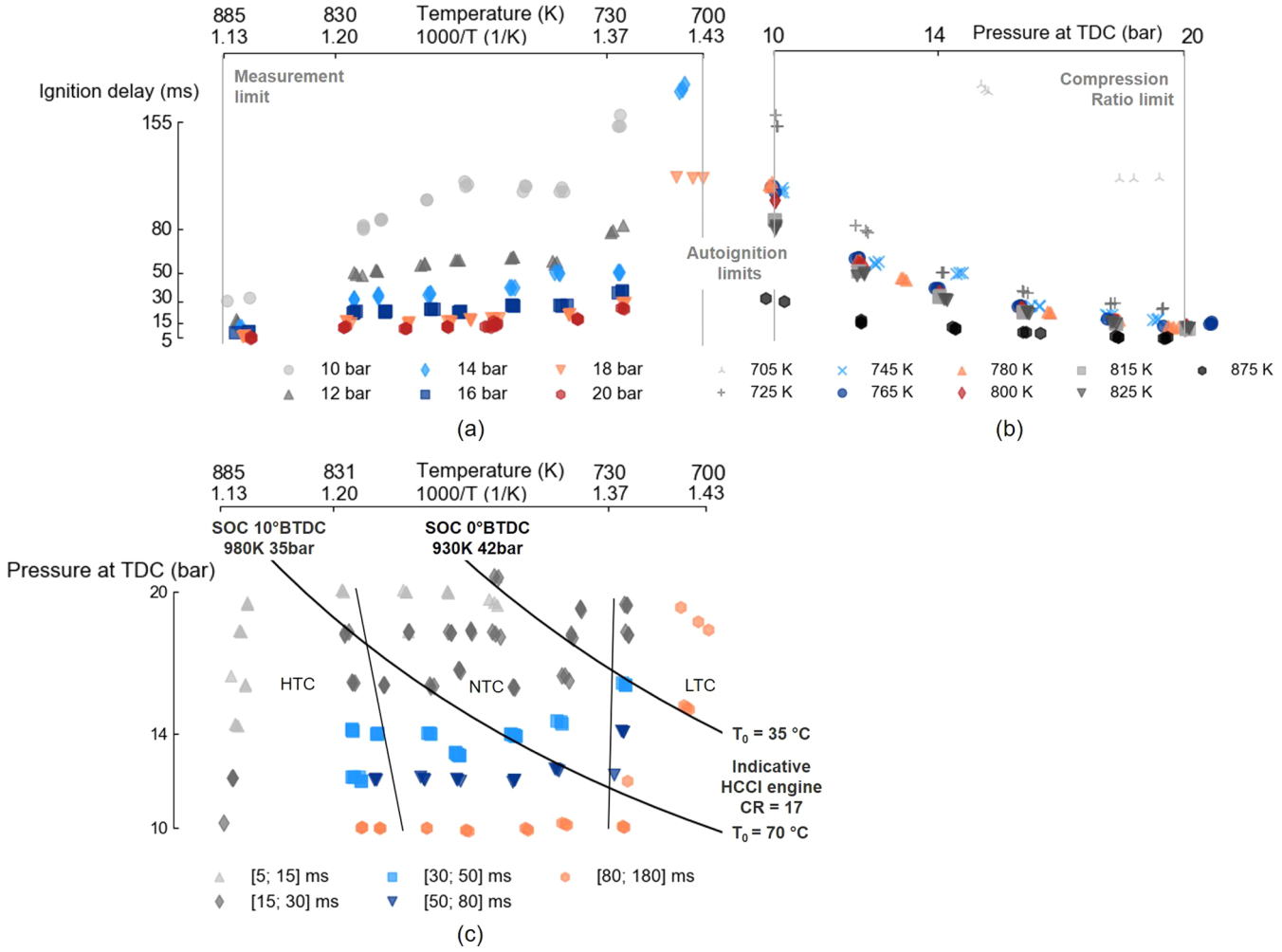

Figure 3. Investigated conditions and measured main-stage IDs. The achieved temperatures were calculated on the basis of the estimated mean value of the heat capacity. The range of investigated conditions is wide, as shown in panel c. On the same panel, two illustrative HCCI temperature−pressure traces show a range of operating conditions, where a meaningful indicative interval of start of combustion (SOC) timing is achieved. These indicative lines were obtained by calculating the heat losses as advised by Broekaert et al.[55] and Pochet et al.,[56] and the SOC was estimated on the basis of extrapolated ignition delays and the knock integral model (KIM) studied by Shahbakhti et al.[57,58]

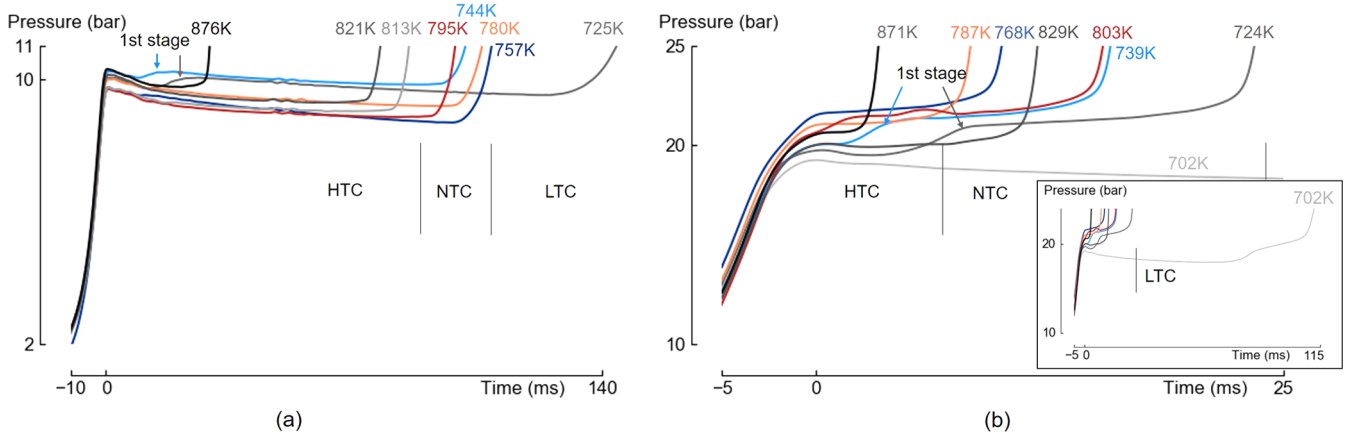

Figure 4. Pressure profiles at 10 bar (9.80 ± 0.4 bar) and 20 bar (19.75 ± 0.9 bar). The high-temperature chemistry (HTC), NTC, and low-temperature chemistry (LTC) regions were defined according to the changes of slopes in Figure 5.

RESULTS AND DISCUSSION

Overall, the results presented below report the investigated conditions, the ignition limits, and the NTC zone characteristics and discuss the fuel ignition. Throughout this section, we use the terms "slope", "intensity", and "temperature coefficient" E/R interchangeably.

Ignition Delays. The fuel has a standard behavior governed by the basics of the combustion chemistry under

DOI: 10.1021/acs.energyfuels.9b00649
Energy Fuels 2019, 33, 5664−5672

low, intermediate, and high temperatures. To cover these conditions jointly with the pressure effect, we tested 10 reactive mixtures (one mixture per temperature) with an equivalence ratio of 0.5 ± 0.0045, varying the pressure and temperature at TDC from 9.8 ± 0.4 to 21.4 ± 0.2 bar and from 705.1 ± 1.6 to 878.4 ± 3.5 K, respectively (Figure 3). All of the data are provided in the Supporting Information.

Two HCCI compression curves were plotted in Figure 3c, with two different initial temperatures, allowing for a meaningful start of ignition (SOI) under the HCCI mode. These traces show that, with a well-chosen compression ratio, the required range of temperatures does not require a stringent preheating system to run under a HCCI engine. Moreover, the studied conditions are relevant and cover the pressure and temperature achieved during a HCCI compression stroke at an equivalence ratio of 0.5.

The lowest investigated temperature and pressure correspond to the ignition limit, while measuring an ID at higher temperatures or pressures would have led to very short and unmeasurable IDs. The measured IDs (from 5 to 155 ms, with a maximum reaching 193.8 ms) show conventional features.

First, the IDs decrease exponentially when the temperature increases and according to a power law P^n with pressure (Figure 3), with a deviation from Arrhenius behavior. This deviation corresponds to a temperature zone where the temperature coefficient E/R in the Arrhenius law decreases and can be negative, meaning that the rate at which the reactivity increases with the temperature is reduced. This NTC is a consequence of a competition between two different kinetic pathways, i.e., low-temperature chain-branching pathways and intermediate-temperature chain-terminating pathways, as described by Battin-Leclerc.[59]

Second, two-stage ignition was observed between 705 and 750 K, where a first pressure rise, also known as first-stage ignition, takes place before the main ignition (Figure 4). Long alkyl chain molecules can produce ketohydroperoxides, the chain-branching agents responsible for the appearance of first-stage ignition. The chain-branching pathways of alkanes typically proceed through addition of an alkyl radical to O_2 and further isomerization to hydroperoxides to ultimately yield ketohydroperoxides. With the increase of the temperature in this constant volume experiment, the first-stage of ignition promotes reactivity and decreases the total ignition delay.

Third, as the pressure increases, the temperature coefficient increases (Figure 5). This phenomenon is explained by the rates of formation and consumption of the intermediates that promote reactivity in the LTC (hydroperoxides) and NTC zones, respectively. Intermediate-temperature chain branching through decomposition of hydrogen peroxide begins as the temperature reaches the NTC conditions; consequently, the low-temperature reactivity weakens. The extent of the NTC behavior and associated temperature range is therefore directly correlated to the propensity of a fuel to form hydroperoxides and/or hydrogen peroxide. The decrease of the NTC extent with the pressure that was previously described can be explained by the facilitated decomposition of hydrogen peroxide into two OH radicals under higher pressures.[39] In the chemical equation H_2O_2 (+M) = OH + OH (+M), where M is the third body in the reaction expression, any increase in pressure will lead to a significant increase of the reaction rate.

This fuel displays two-stage ignition behavior as well as a deviation from Arrhenius law. However, the temperature coefficient, i.e., the slope in the NTC zone, remains positive,

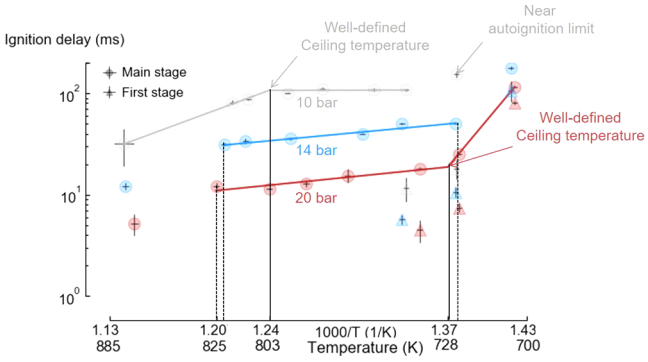

Figure 5. IDs at an equivalence ratio of 0.5 ± 0.0045 for three pressures, 19.75 ± 0.9, 14.55 ± 0.6, and 9.80 ± 0.4 bar, and three types of ignition regimes, high-temperature, NTC, and low-temperature zones. The main and first-stage ignitions are symbolized by circles and triangles, respectively. The error bars represent the combined uncertainty extended at 95%, taking into account both the repeatability and the C_p uncertainties and calculated following the *Evaluation of Measurement Data—Guide to the Expression of Uncertainty in Measurement*.[53] The straight lines were drawn when enough data were available to define the limits between the LTC, NTC, and HTC regions.

probably because of the low paraffin fraction. This has been observed before in the case of alkane/alkene mixtures.[60]

Atypical Behavior. In this section, the specificities of the studied fuel reactivity are identified by comparing the ignition delays to two multicomponent surrogate fuels proposed by KAUST, i.e., FGG-KAUST and FGI-KAUST. Then, the identified specificities are discussed with regard to the molecular composition. FACE G (surrogate FGG-KAUST) and FACE I (surrogate FGI-KAUST) define a good framework because the first has high ignition delays, while the second is a highly reactive gasoline fuel.[26,27]

The following observations show that the studied fuel is characterized by high reactivity under intermediate temperatures but very limited reactivity under low temperatures (Figure 6). First, the ASR fuel shows a reactivity of the same

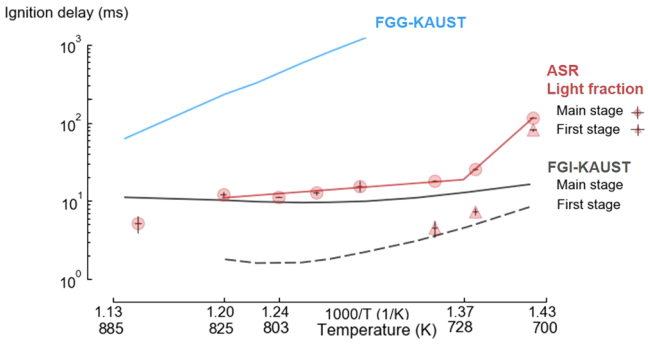

Figure 6. ASR fuel ignition delays at 20 bar and at an equivalence ratio of 0.5 compared to the KAUST surrogate fuels for FACE G and FACE I, i.e., FGG-KAUST and FGI-KAUST.[26,27] The reactivity in the NTC region is similar to the reactivity of FGI-KAUST.

order of magnitude (ignition delay of about 10 ms) as the reactivity of FGI-KAUST in the NTC area but decreases dramatically when the NTC/LTC ceiling temperature is crossed. At a low temperature, the autoignition vanishes, even if the ignition delay is still relatively low compared to the relatively of FGG-KAUST (100 ms). Last but not least,

DOI: 10.1021/acs.energyfuels.9b00649
Energy Fuels 2019, 33, 5664−5672

Table 4. Distinctive Aromatic Groups Defined by Roubaud et al.[64]

group	toluene	*o*-xylene	styrene
molecules	toluene	ethylbenzene	styrene
	1,3,5-trimethylbenzene	1,2,3-trimethylbenzene	α-methylstyrene
	xylene (*m*- and *p*-)		
mole fraction (%)	5.72	6.34	8.68

conversely to FGI-KAUST, the first-stage ignition is only visible when the compressed temperature is lower than 750 K, which shows that a small number of low-temperature chain-branching intermediates are formed because they cannot compete with the NTC reaction pathways.

This fuel includes a large olefinic portion (29.61%, mol/mol; Table 2), molecules that are generally characterized by a low reactivity under low temperatures.[61,62] 2,4-Dimethyl-1-heptene is the olefinic molecule with the higher fraction and is likely to display reaction pathways relevant to alkenes and alkanes because of its double bond yielding a total of five allylic H-abstraction sites as well as its long alkyl chain. Allylic hydroperoxydes are not favorable for the addition to O_2 molecules, even though allylic radicals can recombine with HO_2 radicals to form allylic peroxides.[63] The alkylic section of this molecule is branched, which will be detrimental to the internal isomerization of potential RO_2 adducts. To summarize, the long molecule length promotes the reactivity; nevertheless, the limited alkylic isomerization possibilities and the allylic sites limit the low-temperature reactivity.

A large portion of aromatics is also present in the fuel with almost 25%, mol/mol (Table 2), split into three subgroups: the toluene-, *o*-xylene-, and styrene-like groups. Roubaud et al. demonstrated that *o*-xylene as well as long-chain aromatics react at low temperatures[64] following two-stage ignition, under high-pressure conditions. Toluene easily forms the resonance-stabilized benzyl radical, which is an important radical scavenger in the low-temperature region.[39] Because all of its C−H bonds are either benzenic or vinylic with high bond dissociation energies, styrene is likely to combine ignition resistance characteristics associated with toluene and short-chain alkenes. The studied fuel is characterized by a higher fraction of aromatics belonging to the two groups that does not react in the low-temperature region, explaining its low reactivity in this region (Table 4).

The high aromatic fraction can also explain the high difference of reactivity between the LTC and NTC. Because of the formation of resonance-stabilized radicals, abstraction of hydrogen by O_2 or HO_2 is favored, facilitating the formation of hydrogen peroxide. Intermediate temperature reactivity is therefore favored, in accordance with the significant octane sensitivity usually observed for these fuels.

Finally, a significant portion of this fuel is composed of a high number of oxygenated molecules (25 molecules and 18 isomers identified). In a previous study, 6.8% of oxygenates had been detected by GC × GC, but 16% was estimated after applying a correction.[12] Ketones represent a large contribution to this group. Short ketones are known to display very low reactivity in the low-temperature regime. This is mostly due to the fact that the addition to O_2 by radicals originating from these ketones mostly results in HO_2 elimination to yield unsaturated species, with the formation of peroxides being difficult.[65]

CONCLUSION

The experiments conducted in the present work provide data under HCCI-like conditions to the combustion community for a fuel that had not been studied previously in a RCM. More experimental data for other equivalence ratios, typically 0.3 and 0.8, would provide additional information for operating conditions without exhaust gas recirculation (EGR) and with a high EGR rate.

The fuel showed common features, such as the decrease of the ignition delay with the pressure and temperature, except in a NTC region ($725 < T < 825$ K). The slope of the NTC region decreases with the pressure, and a first-stage ignition was detected near the ceiling temperature between the low-temperature and NTC regions. A more specific attribute was observed: a low reactivity under LTC, explained by the major molecules blended: substituted olefin, aromatics with a reactivity comparable to the reactivity of *o*-xylene, and oxygenates (ketones, alcohols, and benzenoids).

Among the final applications, this study offers a first overview on the reactivity of ASR fuels, which, until now, was unknown. A surrogate fuel could be formulated and validated, although relying on the major constituting molecules of the fuel is impossible, because some of them have never been studied in pure form.

Numerical simulations will lead with this surrogate fuel to the investigation of the potential of HCCI operating conditions to reduce the pollutants emitted by waste-derived fuels.

ASSOCIATED CONTENT

Supporting Information

The Supporting Information is available free of charge on the ACS Publications website at DOI: 10.1021/acs.energyfuels.9b00649.

RCM experimental measurements (IgnitionDelays), non-reactive volume profiles (NonReactiveVolProfile), mean values of the molecule mole fractions calculated with the mass fractions over three GC × GC runs (GCGC_mean), mass fractions for each of these runs (GCGC_raw), NASA coefficients to calculate the evaluated minimal, mean, and maximal fuel heat capacities from 0 to 1000 K (NASA_coefficients), and molecular database that was used to estimate the fuel heat capacity (Database_to_calculate_NASA_coef) (XLSX)

AUTHOR INFORMATION

Corresponding Author

*E-mail: steven.tipler@ulb.ac.be.

ORCID

S. Tipler: 0000-0002-0964-5038

F. Contino: 0000-0002-8341-4350

DOI: 10.1021/acs.energyfuels.9b00649
Energy Fuels 2019, 33, 5664−5672

Notes

The authors declare no competing financial interest.

■ ACKNOWLEDGMENTS

The authors thank the staff from the Physicochimie des Processus de Combustion et de l'Atmosphère (PC2A) laboratory, Université de Lille (particularly P. Demaux and H. Kechmir) for their technical help during the experiments. Thanks are also due to Steffen H. Symoens, Marko R. Djokic, and Kevin M. Van Geem from the Laboratory for Chemical Technology of Ghent University, who previously lead the comprehensive two-dimensional gas chromatography measurements and post-treatment and who also provided their precious knowledge on this technology. This work was carried out within the framework of an EU project and benefited from a grant from la Région Wallonne.

■ REFERENCES

(1) European Commission (EC). *End-of-Life Vehicle Statistics*; EC: Brussels, Belgium, 2018.
(2) Cossu, R.; Lai, T. Automotive shredder residue (ASR) management: An overview. *Waste Manage.* **2015**, *45*, 143−151.
(3) Rey, L.; Conesa, J. A.; Aracil, I.; Garrido, M. A.; Ortuño, N. Pollutant formation in the pyrolysis and combustion of Automotive Shredder Residue. *Waste Manage.* **2016**, *56*, 376−383.
(4) InnovaTech. *Projet Phoenix—Une Magnifique Vitrine Technologique pour la Wallonie*; InnovaTech: Rockford, IL, 2013.
(5) Jody, B. J.; Daniels, E. J.; Duranceau, C. M.; Pomykala, J. A.; Spangenberger, J. S. *End-of-Life Vehicle Recycling: State of the Art of Resource Recovery from Shredder Residue*; Energy Systems Division, Argonne National Laboratory: Argonne, IL, 2011; ANL/ESD/07-8.
(6) Ichikawa, M.; Nonaka, N.; Amano, H.; Takada, I.; Ishimori, S.; Andoh, H.; Kumamoto, K. Proton NMR Analysis of Octane Number for Motor Gasoline: Part IV. *Appl. Spectrosc.* **1992**, *46*, 498−503.
(7) Ichikawa, M.; Nonaka, N.; Amano, H.; Takada, I.; Ishimori, S. Proton NMR Analysis of Octane Number for Motor Gasoline: Part II. *Appl. Spectrosc.* **1991**, *45*, 637−640.
(8) Council of European Union.. Directive 2009/30/EC of the European Parliament and of the Council of 23 April 2009 amending Directive 98/70/EC as regards the specification of petrol, diesel and gas-oil and introducing a mechanism to monitor and reduce greenhouse gas emissions and amending Council Directive 1999/32/EC as regards the specification of fuel used by inland waterway vessels and repealing Directive 93/12/EEC. *Off. J. Eur. Union* **2009**, *52*, 88−113.
(9) Štrumberger, N.; Gospočić, A.; Hvu, M.; Bartulić, Č. Polymeric materials in automobiles. *Promet—Traffic—Traffico* **2005**, *17*, 149−160.
(10) Sarker, M.; Rashid, M. M.; Molla, M.; Rahman, M. S. Thermal Conversion of Waste Plastics (HDPE, PP and PS) to Produce Mixture of Hydrocarbons. *Am. J. Environ. Eng.* **2012**, *2*, 128−136.
(11) Guibet, J.-C. *Carburants et Moteurs Technologies, Énergie, Environnement Tome 1*; Editions Technip: Paris, France, 1997.
(12) Tipler, S.; Symoens, S. H.; Djokic, M. R.; Van Geem, K. M.; Parente, A.; Contino, F.; Coussement, A. Prediction of the PIONA and oxygenate composition of unconventional fuels with the Pseudo-Component Property Estimation (PCPE) method. Application to an Automotive Shredder Residues-derived gasoline. *SAE Tech. Pap. Ser.* **2018**, dfg DOI: 10.4271/2018-01-0905.
(13) Mani, M.; Nagarajan, G.; Sampath, S. Characterisation and effect of using waste plastic oil and diesel fuel blends in compression ignition engine. *Energy* **2011**, *36*, 212−219.
(14) Kumar, S.; Prakash, R.; Murugan, S.; Singh, R. K. Performance and emission analysis of blends of waste plastic oil obtained by catalytic pyrolysis of waste HDPE with diesel in a CI engine. *Energy Convers. Manage.* **2013**, *74*, 323−331.
(15) Contino, F.; Dagaut, P.; Halter, F.; Masurier, J.-B.; Dayma, G.; Mounaïm-Rousselle, C.; Foucher, F. Screening Method for Fuels in Homogeneous Charge Compression Ignition Engines: Application to Valeric Biofuels. *Energy Fuels* **2017**, *31*, 607−614.
(16) Bhaduri, S.; Berger, B.; Pochet, M.; Jeanmart, H.; Contino, F. HCCI engine operated with unscrubbed biomass syngas. *Fuel Process. Technol.* **2017**, *157*, 52−58.
(17) Pochet, M.; Dias, V.; Jeanmart, H.; Verhelst, S.; Contino, F. Multifuel CHP HCCI Engine towards Flexible Power-to-fuel: Numerical Study of Operating Range. Energy Procedia. 2017. *Energy Procedia* **2017**, *105*, 1532−1538.
(18) An, Y.; Jaasim, M.; Raman, V.; Hernández Pérez, F. E.; Sim, J.; Chang, J.; Im, H. G.; Johansson, B. Homogeneous charge compression ignition (HCCI) and partially premixed combustion (PPC) in compression ignition engine with low octane gasoline. *Energy* **2018**, *158*, 181−191.
(19) Pochet, M.; Dias, V.; Moreau, B.; Foucher, F.; Jeanmart, H.; Contino, F. Experimental and numerical study, under LTC conditions, of ammonia ignition delay with and without hydrogen addition. *Proc. Combust. Inst.* **2019**, *37*, 621−629.
(20) Pochet, M.; Truedsson, I.; Foucher, F.; Jeanmart, H.; Contino, F. Ammonia-Hydrogen Blends in Homogeneous-Charge Compression-Ignition Engine. *SAE Tech. Pap. Ser.* **2017**, DOI: 10.4271/2017-24-0087.
(21) Pitz, W. J.; Mueller, C. J. Recent progress in the development of diesel surrogate fuels. *Prog. Energy Combust. Sci.* **2011**, *37*, 330−350.
(22) Yu, J.; Ju, Y.; Gou, X. Surrogate fuel formulation for oxygenated and hydrocarbon fuels by using the molecular structures and functional groups. *Fuel* **2016**, *166*, 211−218.
(23) Pera, C.; Knop, V. Methodology to define gasoline surrogates dedicated to auto-ignition in engines. *Fuel* **2012**, *96*, 59−69.
(24) Ahmed, A.; Goteng, G.; Shankar, V. S. B.; Al-Qurashi, K.; Roberts, W. L.; Sarathy, S. M. A computational methodology for formulating gasoline surrogate fuels with accurate physical and chemical kinetic properties. *Fuel* **2015**, *143*, 290−300.
(25) Sarathy, S. M.; Kukkadapu, G.; Mehl, M.; Wang, W.; Javed, T.; Park, S.; Oehlschlaeger, M. A.; Farooq, A.; Pitz, W. J.; Sung, C. J. Ignition of alkane-rich FACE gasoline fuels and their surrogate mixtures. *Proc. Combust. Inst.* **2015**, *35*, 249−257.
(26) Sarathy, S. M.; Kukkadapu, G.; Mehl, M.; Javed, T.; Ahmed, A.; Naser, N.; Tekawade, A.; Kosiba, G.; AlAbbad, M.; Singh, E.; Park, S.; Rashidi, M. A.; Chung, S. H.; Roberts, W. L.; Oehlschlaeger, M. A.; Sung, C.-J.; Farooq, A. Compositional effects on the ignition of FACE gasolines. *Combust. Flame* **2016**, *169*, 171−193.
(27) Javed, T.; Ahmed, A.; Lovisotto, L.; Issayev, G.; Badra, J.; Sarathy, S. M.; Farooq, A. Ignition studies of two low-octane gasolines. *Combust. Flame* **2017**, *185*, 152−159.
(28) Javed, T.; Nasir, E. F.; Ahmed, A.; Badra, J.; Djebbi, K.; Beshir, M.; Ji, W.; Sarathy, S. M.; Farooq, A. Ignition delay measurements of light naphtha: A fully blended low octane fuel. *Proc. Combust. Inst.* **2017**, *36*, 315−322.
(29) Alabbad, M.; Issayev, G.; Badra, J.; Voice, A. K.; Giri, B. R.; Djebbi, K.; Ahmed, A.; Sarathy, S. M.; Farooq, A. Autoignition of straight-run naphtha: A promising fuel for advanced compression ignition engines. *Combust. Flame* **2018**, *189*, 337−346.
(30) Chang, J.; Viollet, Y.; Amer, A.; Kalghatgi, G. Fuel Economy Potential of Partially Premixed Compression Ignition (PPCI) Combustion with Naphtha Fuel. *SAE Tech. Pap. Ser.* **2013**, DOI: 10.4271/2013-01-2701.
(31) Chang, J.; Kalghatgi, G.; Amer, A.; Viollet, Y. Enabling High Efficiency Direct Injection Engine with Naphtha Fuel through Partially Premixed Charge Compression Ignition Combustion. *SAE Tech. Pap. Ser.* **2012**, DOI: 10.4271/2012-01-0677.
(32) Badra, J. A.; Bokhumseen, N.; Mulla, N.; Sarathy, S. M.; Farooq, A.; Kalghatgi, G.; Gaillard, P. A methodology to relate octane numbers of binary and ternary *n*-heptane, iso-octane and toluene mixtures with simulated ignition delay times. *Fuel* **2015**, *160*, 458−469.

DOI: 10.1021/acs.energyfuels.9b00649
Energy Fuels 2019, 33, 5664−5672

(33) Naser, N.; Yang, S. Y.; Kalghatgi, G.; Chung, S. H. Relating the octane numbers of fuels to ignition delay times measured in an ignition quality tester (IQT). *Fuel* **2017**, *187*, 117−127.
(34) Naser, N.; Sarathy, S. M.; Chung, S. H. Ignition delay time sensitivity in ignition quality tester (IQT) and its relation to octane sensitivity. *Fuel* **2018**, *233*, 412−419.
(35) Leppard, W. R. The Chemical Origin of Fuel Octane Sensitivity. *SAE Tech. Pap. Ser.* **1990**, DOI: 10.4271/902137.
(36) Jarrosson, F.; Fenard, Y.; Vanhove, G.; Dauphin, R. Gasoline and Combustion: Relationship between Molecular Structure and Performance. *SAE Tech. Pap. Ser.* **2018**, DOI: 10.4271/2018-01-0906.
(37) Zádor, J.; Taatjes, C. A.; Fernandes, R. X. Kinetics of elementary reactions in low-temperature autoignition chemistry. *Prog. Energy Combust. Sci.* **2011**, *37*, 371−421.
(38) Curran, H. J. Developing detailed chemical kinetic mechanisms for fuel combustion. *Proc. Combust. Inst.* **2019**, *37*, 57−81.
(39) Vanhove, G.; Petit, G.; Minetti, R. Experimental study of the kinetic interactions in the low-temperature autoignition of hydrocarbon binary mixtures and a surrogate fuel. *Combust. Flame* **2006**, *145*, 521−532.
(40) Boot, M. D.; Tian, M.; Hensen, E. J.; Mani Sarathy, S. Impact of fuel molecular structure on auto-ignition behavior—Design rules for future high performance gasolines. *Prog. Energy Combust. Sci.* **2017**, *60*, 1−25.
(41) Ristic, N. D.; Djokic, M. R.; Konist, A.; Van Geem, K. M.; Marin, G. B. Quantitative compositional analysis of Estonian shale oil using comprehensive two dimensional gas chromatography. *Fuel Process. Technol.* **2017**, *167*, 241−249.
(42) Dijkmans, T.; Djokic, M. R.; Van Geem, K. M.; Marin, G. B. Comprehensive compositional analysis of sulfur and nitrogen containing compounds in shale oil using GC × GC−FID/SCD/NCD/TOF−MS. *Fuel* **2015**, *140*, 398−406.
(43) Lee, C.; Ahmed, A.; Nasir, E. F.; Badra, J.; Kalghatgi, G.; Sarathy, S. M.; Curran, H.; Farooq, A. Autoignition characteristics of oxygenated gasolines. *Combust. Flame* **2017**, *186*, 114−128.
(44) Riazi, M. R. *Statewide Agricultural Land Use Baseline 2015*; ASTM International: West Conshohocken, PA, 2005.
(45) Kurtz, S.; Ward, A. The refractivity intercept and the specific refraction equation of Newton. I. Development of the refractivity intercept and comparison with specific refraction equations. *J. Franklin Inst.* **1936**, *222*, 563−592.
(46) ASTM International. *ASTM D4052-18, Standard Test Method for Density, Relative Density, and API Gravity of Liquids by Digital Density Meter*; ASTM International: West Conshohocken, PA, 2018.
(47) Fenard, Y.; Boumehdi, M.; Vanhove, G. Experimental and kinetic modeling study of 2-methyltetrahydrofuran oxidation under engine-relevant conditions. *Combust. Flame* **2017**, *178*, 168−181.
(48) Goldsborough, S. S.; Hochgreb, S.; Vanhove, G.; Wooldridge, M. S.; Curran, H. J.; Sung, C.-J. Advances in rapid compression machine studies of low- and intermediate-temperature autoignition phenomena. *Prog. Energy Combust. Sci.* **2017**, *63*, 1−78.
(49) Lee, D.; Hochgreb, S. Rapid compression machines: Heat transfer and suppression of corner vortex. *Combust. Flame* **1998**, *114*, 531−545.
(50) Khandal, S. V.; Banapurmath, N. R.; Gaitonde, V. N. Performance studies on homogeneous charge compression ignition (HCCI) engine powered with alternative fuels. *Renewable Energy* **2019**, *132*, 683−693.
(51) Wang, Z.; Liu, H.; Ma, X.; Wang, J.; Shuai, S.; Reitz, R. D. Homogeneous charge compression ignition (HCCI) combustion of polyoxymethylene dimethyl ethers (PODE). *Fuel* **2016**, *183*, 206−213.
(52) Nishi, M.; Kanehara, M.; Iida, N. Assessment for innovative combustion on HCCI engine by controlling EGR ratio and engine speed. *Appl. Therm. Eng.* **2016**, *99*, 42−60.
(53) Joint Committee for Guides in Metrology (JCGM). *Evaluation of Measurement Data—Guide to the Expression of Uncertainty in Measurement*; International Organization for Standardization (ISO): Geneva, Switzerland, 2008; JCGM 100:2008.
(54) Bourgeois, N.; Goldsborough, S. S.; Vanhove, G.; Duponcheel, M.; Jeanmart, H.; Contino, F. CFD simulations of Rapid Compression Machines using detailed chemistry: Impact of multi-dimensional effects on the auto-ignition of the iso-octane. *Proc. Combust. Inst.* **2017**, *36*, 383−391.
(55) Broekaert, S.; De Cuyper, T.; Chana, K.; De Paepe, M.; Verhelst, S. Assessment of Empirical Heat Transfer Models for a CFR Engine Operated in HCCI Mode. *SAE Tech. Pap. Ser.* **2015**, DOI: 10.4271/2015-01-1750.
(56) Pochet, M.; Dias, V.; Jeanmart, H.; Verhelst, S.; Contino, F. Multifuel CHP HCCI Engine towards Flexible Power-to-fuel: Numerical Study of Operating Range. *Energy Procedia* **2017**, *105*, 1532−1538.
(57) Shahbakhti, M.; Lupul, R.; Koch, C. R. Predicting HCCI Auto-Ignition Timing by Extending a Modified Knock-Integral Method. *SAE Tech. Pap. Ser.* **2007**, DOI: 10.4271/2007-01-0222.
(58) Shahbakhti, M.; Lupul, R.; Koch, C. R. Sensitivity analysis & modeling of HCCI auto-ignition timing. *IFAC Proc. Vol.* **2007**, *40*, 303−310.
(59) Battin-Leclerc, F. Detailed chemical kinetic models for the low-temperature combustion of hydrocarbons with application to gasoline and diesel fuel surrogates. *Prog. Energy Combust. Sci.* **2008**, *34*, 440−498.
(60) Vanhove, G.; Minetti, R.; Touchard, S.; Fournet, R.; Glaude, P.; Battin-Leclerc, F. Experimental and modeling study of the auto-ignition of 1-hexene/isooctane mixtures at low temperatures. *Combust. Flame* **2006**, *145*, 272−281.
(61) Vanhove, G.; Ribaucour, M.; Minetti, R. On the influence of the position of the double bond on the low-temperature chemistry of hexenes. *Proc. Combust. Inst.* **2005**, *30*, 1065−1072.
(62) Mehl, M.; Vanhove, G.; Pitz, W. J.; Ranzi, E. Oxidation and combustion of the *n*-hexene isomers: A wide range kinetic modeling study. *Combust. Flame* **2008**, *155*, 756−772.
(63) Goldsmith, C. F.; Green, W. H.; Klippenstein, S. J. Role of O_2 + QOOH in Low-Temperature Ignition of Propane. 1. Temperature and Pressure Dependent Rate Coefficients. *J. Phys. Chem. A* **2012**, *116*, 3325−3346.
(64) Roubaud, A.; Minetti, R.; Sochet, L. Oxidation and combustion of low alkylbenzenes at high pressure: Comparative reactivity and auto-ignition. *Combust. Flame* **2000**, *121*, 535−541.
(65) Burke, U.; Beeckmann, J.; Kopp, W. A.; Uygun, Y.; Olivier, H.; Leonhard, K.; Pitsch, H.; Heufer, K. A. A comprehensive experimental and kinetic modeling study of butanone. *Combust. Flame* **2016**, *168*, 296−309.

DOI: 10.1021/acs.energyfuels.9b00649
Energy Fuels 2019, 33, 5664−5672